Talanta 124 (2014) 36–42

Contents lists available at ScienceDirect

Talanta

journal homepage: www.elsevier.com/locate/talanta

Short communication

A non-linearity criterion applied to the calibration curve method involved with ion-selective electrodes

Tadeusz Michałowski [a,*], Bogusław Pilarski [b], Anna M. Michałowska-Kaczmarczyk [c], Agata Kukwa [b]

[a] Faculty of Engineering and Chemical Technology, Technical University of Cracow, 31-155 Cracow, Poland
[b] Cerko Sp. z o.o. Sp.K., 81-451 Gdynia, Al. Zwycięstwa 96/98, Poland
[c] Department of Oncology, The University Hospital in Cracow, 31-501 Cracow, Poland

ARTICLE INFO

Article history:
Received 25 November 2013
Received in revised form
1 February 2014
Accepted 13 February 2014
Available online 20 February 2014

Keywords:
Potentiometric titration
ISE calibration
Curve fitting
Rational functions

ABSTRACT

Some rational functions of the Padé type, $y=y(x; n,m)$, were applied to the calibration curve method (CCM), and compared with a parabolic function. The functions were tested on the results obtained from calibration of ion-selective electrodes: NH_4-ISE, Ca-ISE, and F-ISE. A validity of the functions $y=y(x; 2,1)$, $y=y(x; 1,1)$, and $y=y(x; 2,0)$ (parabolic) was compared. A uniform, integral criterion of nonlinearity of calibration curves is suggested. This uniformity is based on normalization of the approximating functions within the frames of a unit area.

1. Introduction

In the calibration curve method (CCM), commonly considered as the preliminary step in different methods of chemical analysis, the linear functions are usually applied. The degree of linearity of such lines is expressed by the coefficient of determination R^2 (squared linear correlation coefficient, R) value [1]. When referred to nonlinear relationships, except the nonlinear correlation coefficient [2], there are no valuable manners of such an evaluation; it particularly refers to curvilinear relationships approximated by rational functions of the Padé type [3–5], expressed as the ratio of two polynomial functions $P_n(x)$ and $Q_m(x)$, of nth and mth degree, respectively [6]

$$y = y(x; n, m) = \frac{P_n(x)}{Q_m(x)} \tag{1}$$

The Padé approximants still attract attention of physicists and mathematicians; an extensive list of the related papers is provided in [7]. It was found that various experimental data can be elegantly modeled with use of rational functions [8–14].

The functions of the Padé type appeared to be a valuable tool for modeling the titration curves referred to complex acid–base systems; see [15,16] and other references cited therein, or to a complex redox system [17]. There were shown that rational functions provide much better approximation than polynomial functions with the same number of parameters involved, expressed in terms of natural or converted variables [18–22]. This method is computationally efficient and manifests a high robustness [6,23]. The Padé approximants are now employed in diverse contexts, indicated in [24].

This paper refers to the normalization of calibration curves applied for determination of some ions: NH_4^+, Ca^{2+} and F^-, with use of ion-selective electrodes (ISEs), within defined ranges of concentrations of particular ions. Nonlinearity of the curves within these ranges is measured according to an integral criterion of nonlinearity, with use of rational and parabolic functions. Applicability of particular functions for modeling purposes has also been taken into account.

2. Some rational functions and normalization principle

Let us refer first to the rational function (A-model)

$$y = \frac{a_0 + a_1 \cdot x + a_2 \cdot x^2}{1 + a_3 \cdot x} \tag{2}$$

* Correspondence to: Faculty of Chemical Engineering and Technology, Cracow University of Technology, Warszawska 24, 31-155 Cracow, Poland. Tel.: +48 12 628 21 77.
E-mail address: michalot@o2.pl (T. Michałowski).

http://dx.doi.org/10.1016/j.talanta.2014.02.027
0039-9140

Nomenclature

CCM	Calibration curve method
D	Titrand
ISE	Ion-selective electrode
LSM	Least squares method
T	Titrant

i.e., $n=2$ and $m=1$ in Eq. (1). On this basis, one can also consider some simplified forms of Eq. (2), referred to the options: $a_2=0$ (B-model), or $a_3=0$ (C-model). In particular, for the C-model we get the parabolic function

$$y = a_0 + a_1 \cdot x + a_2 \cdot x^2 \tag{3}$$

where $Q_m=Q_0=1$. Function (2) and its simplified forms will be applied for CCM purposes.

Let us take the set of experimental data $\{(x_j, y_j) \mid j=1,\ldots,N\}$, where $x_1 < x_2 < \ldots < x_N$. Denoting $\Delta x = x_N - x_1$ and $\Delta y = y_N - y_1$, for the monotonic function ($y_j \langle y_{j+1}$ or $y_j \rangle y_{j+1}$ at $j=1,\ldots, N-1$), we introduce the variables u and v through the relations:

$$x = x_1 + u \cdot \Delta x \text{ and } y = y_1 + v \cdot \Delta y \tag{4}$$

Applying them to function (2), after a lengthy but straightforward algebra, we get the relation for the A-model (see Appendix A)

$$v = v(u) = \frac{\alpha \cdot u + \beta \cdot u^2}{1 + \gamma \cdot u} \tag{5}$$

where

$$\alpha = \frac{(a_1 + 2a_2 \cdot x_1 - a_3 y_1)}{1 + a_3 x_1} \cdot \frac{\Delta x}{\Delta y} \tag{6}$$

$$\beta = \frac{a_2}{1 + a_3 x_1} \cdot \frac{(\Delta x)^2}{\Delta y} \tag{7}$$

$$\gamma = \frac{a_3}{1 + a_3 x_1} \cdot \Delta x \tag{8}$$

Note that $v(0)=0$. At $(u, v)=(1, 1)$, we have the relation

$$\alpha + \beta = 1 + \gamma, \text{ i.e. } \gamma = \alpha + \beta - 1 \tag{9}$$

The parameters $a_0, \ldots, a_3$ in Eqs. (6)–(8) are obtained according to the least squares method (LSM) applied to the regression equation

$$y_j = a_0 + a_1 \cdot x_j + a_2 \cdot x_j^2 - a_3 \cdot x_j \cdot y_j + \varepsilon_j \tag{10}$$

derived from Eq. (2). Note that the formulas (6)–(8) do not involve a_0, and the value $s=\Delta y/\Delta x$, inherent in α and β (Eqs. (6) and (7)), is the mean slope of the curve $y=y(x)$ (Eq. (2)) within the $\langle x_1, x_N \rangle$ interval. For the models B ($a_2=0$), C ($a_3=0$), we have (B) $\beta=0$, (C) $\gamma=0$ respectively. In these cases, Eq. (5) simplifies into the relations [25,26]:

$$\text{B} \quad v = \frac{\alpha \cdot u}{1 + \gamma \cdot u} \text{ (where } \gamma = \alpha - 1) \tag{11}$$

$$\text{(C)} \quad v = \alpha \cdot u + \beta \cdot u^2 \text{ (where } \beta = 1 - \alpha) \tag{12}$$

The relations, Eq. (5) with Eq. (9), Eq. (11) and Eq. (12), are in close relevance to the homotopy problem [27,28].

On the basis of formula (5) or its simpler forms, referred to the models, B and C, any set of experimental points $\{(x_j, y_j) \mid j=1,\ldots,N\}$ in the CCM can be presented within the frames of coordinates (u, v), where $u \in \langle 0, 1 \rangle$ and $v \in \langle 0, 1 \rangle$; see Fig. 1. In all instances, the curve $v=v(u)$ links the points (0, 0) and (1, 1) on the (u, v) plane. A reference is the linear function $y=a_0+a_1 \cdot x$ ($a_2=a_3=0$ in Eq. (2)), where we get the straight line

$$v = u \tag{13}$$

connecting the points (0, 0) and (1, 1) on the (u, v) plane.

In order to use the formulas $v=v(u)$, applicable for calculations made according to tables with elementary integrals, one can apply some transformations of Eqs. (5), (11) and (12); namely, we have (see Appendix A) for the A-model

$$v = \frac{\alpha \cdot u + \beta \cdot u^2}{1 + \gamma \cdot u} = \frac{\beta}{\gamma} \cdot u + \frac{\alpha \cdot \gamma - \beta}{\gamma^2} - \frac{\alpha \cdot \gamma - \beta}{\gamma^3} \cdot \frac{d}{du} \ln\left(u + \frac{1}{\gamma}\right) \tag{14}$$

Putting $\beta=0$ in Eq. (14) we have

$$v = \frac{\alpha \cdot u}{1 + \gamma \cdot u} = \frac{\alpha}{\gamma} - \frac{\alpha}{\gamma^2} \cdot \frac{d}{du} \ln\left(u + \frac{1}{\gamma}\right) \tag{15}$$

for the B-model. Eq. (12), referred to the C-model, needs none preparatory transformation.

3. The integral criterion of nonlinearity

The area between the lines, $v=v(u)$ and $v=u$, plotted in normalized coordinates (u, v), is the measure of nonlinearity of any monotonic relationship obtained on the basis of experimental points $(x_j, y_j) \mid j=1,\ldots,N\}$; see Fig. 1. This area is expressed as follows:

$$\Omega = \int_0^1 |v-u| \cdot du = \begin{cases} \frac{1}{2} - \int_0^1 v \cdot du & \text{for } u \geq v \\ \int_0^1 v \cdot du - \frac{1}{2} & \text{for } v \geq u \end{cases} \tag{16}$$

Then from Eqs. (12), (14) and (15) we get

$$\theta_A = \int_0^1 v \cdot du = \frac{\beta}{2\gamma} + \frac{(\alpha-1)(\alpha+\beta)}{\gamma^2} \cdot \left(1 - \frac{1}{\gamma} \cdot \ln|\alpha+\beta|\right)$$
$$\text{for the A-model, } \gamma = \alpha + \beta - 1 \tag{17}$$

$$\theta_B = \int_0^1 v \cdot du = \frac{\alpha}{\alpha - 1} - \frac{\alpha}{(\alpha-1)^2} \cdot \ln|\alpha| \text{ for the B - model} \tag{18}$$

$$\theta_C = \int_0^1 v \cdot du = \frac{\alpha + 2}{6} \text{ for the C-model} \tag{19}$$

respectively. Then for $u \geq v$ we get

$$\Omega_A = \tfrac{1}{2} - \theta_A, \ \Omega_B = \tfrac{1}{2} - \theta_B \text{ and } \Omega_C = \tfrac{1}{2} - \theta_C$$
$$\text{(see Eq. (16)).} \tag{20}$$

4. Experimental part

4.1. Apparatus and reagents

All the calibration experiments were made according to potentiometric titration mode, with use of ion-selective (1°) ammonium (NH_4-ISE), (2°) calcium (Ca-ISE), and (3°) fluoride (F-ISE) electrodes, purchased in Eutech Instruments. Titrand D and titrant T were freshly prepared in flasks (25 mL) where stock solutions of the corresponding reagents, NH_4Cl, $CaCl_2$, NaF, KCl, CH_3COOH, and CH_3COONa, each of pa purity, were introduced and filled up to the mark with water. Doubly distilled water, with conductivity approximately 0.18 μS/cm, was used for preparation of the solutions and dilutions. In 2°, concentration of KCl (0.1 mol/L) was the same in D and T. In 3°, D and T contained 10 mL of acetate buffer

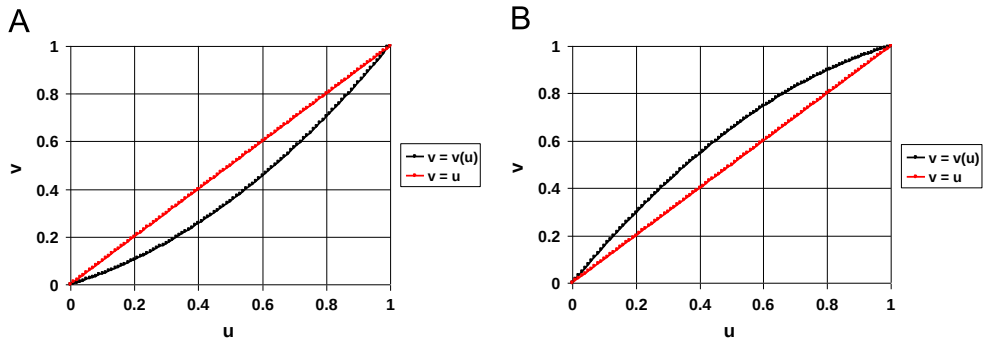

Fig. 1. The plots in (u, v) coordinates at (a) $u \geq v$ and (b) $v \geq u$.

Table 1
Some experimental details involved with the calibrations; C_0, C – concentrations of X_i in D and T, respectively.

i	X-ISE	X_i	V_0 (mL)	C (mol/L)	C_0 (mol/L)	Addition in D and T	*N*
1	NH_4-ISE	NH_4Cl	3	1.215×10^{-3}	1.215×10^{-5}	no addition	300
2	Ca-ISE	$CaCl_2$	2	5×10^{-4}	0	0.1 M KCl	100
3	F-ISE	NaF	2	5×10^{-4}	5×10^{-6}	acetate buffer, pH=5.0	60

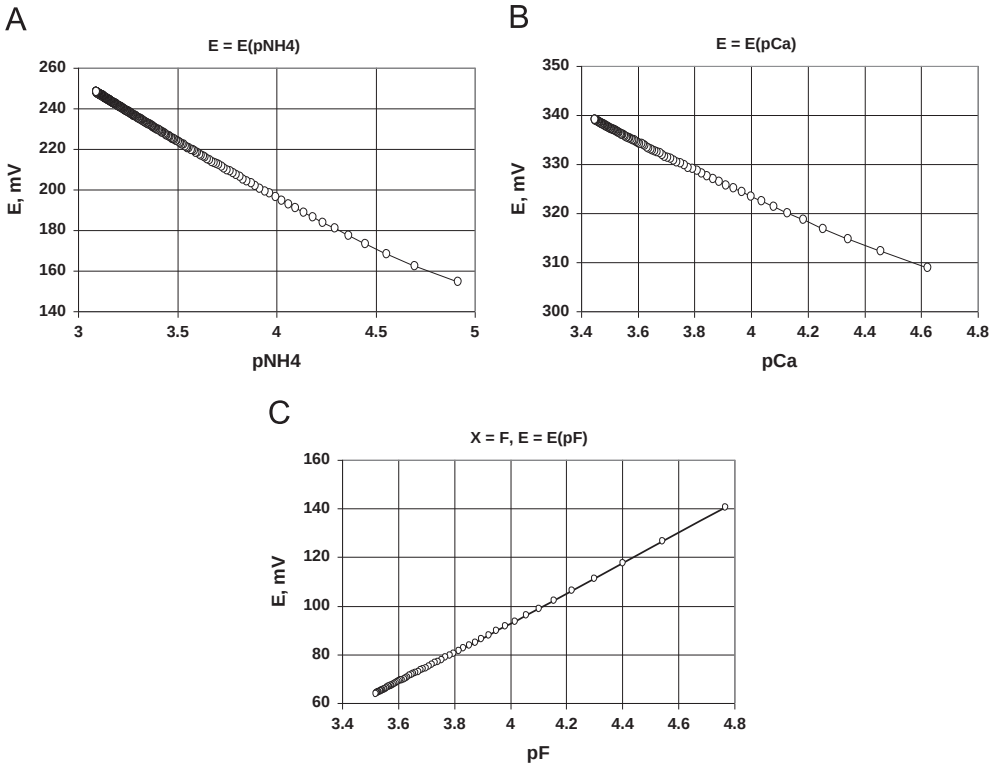

Fig. 2. The curves of (a) $E=E(p\mathrm{NH_4})$ for NH_4-ISE, (b) $E=E(p\mathrm{Ca})$ for Ca-ISE, and (c) $E=E(p\mathrm{F})$ for F-ISE.

(pH=5.0); this buffer was prepared in 25 mL flask by mixing 5.9 mL of 0.2 mol/L acetic acid and 14.1 mL of 0.2 mol/L sodium acetate and filling up to the mark with water. For further experimental details, see Table 1.

The potentiometric titrations were performed in 20 mL measuring cell using a Cerko Lab System (potentiometer resolution ± 0.03 mV) equipped with a Hamilton syringe (5 mL), a magnetic stirrer, temperature-controlled (resistance sensor Pt 1000, ± 0.1 °C) closed system, protected against an effect of carbon dioxide and appropriate ion-selective electrode: (1°) NH_4-ISE, (2°) Ca-ISE, or (3°) F-ISE. The electrodes were conditioned according to Eutech recommendation before each titration. Titrant was added in successive portions 0.050068 mL.

At jth point $(V_j,\ E_j)\,|\,j=1,\ldots,N$ of the titration, E_j [mV] is the potential related to total volume V_j of titrant T (C mol/L X_i) added into V_0 mL of titrand D (C_0 mol/L X_i, see Table 1. Concentrations $[X]_j$ of the corresponding ions in D+T were calculated from the formula

$$[X]_j = (C_0V_0 + CV_j)/(V_0 + V_j),\ pX_j = -\log [X]_j \quad (j = 1, \ldots, N) \qquad (21)$$

We have $[NH_4^+] \gg [NH_3]$ in 1°, $[Ca^{2+}] \gg [CaOH^+]$ in 2°, and $[F^-] \gg [HF]$ in 3°; $[NH_3]/[NH_4^+] = 10^{pH-9.35}$, $[F^-]/[HF] = 10^{pH-3.18}$, and $[CaOH^+]/[Ca^{2+}] = 10^{-12.7+pH}$ [29].

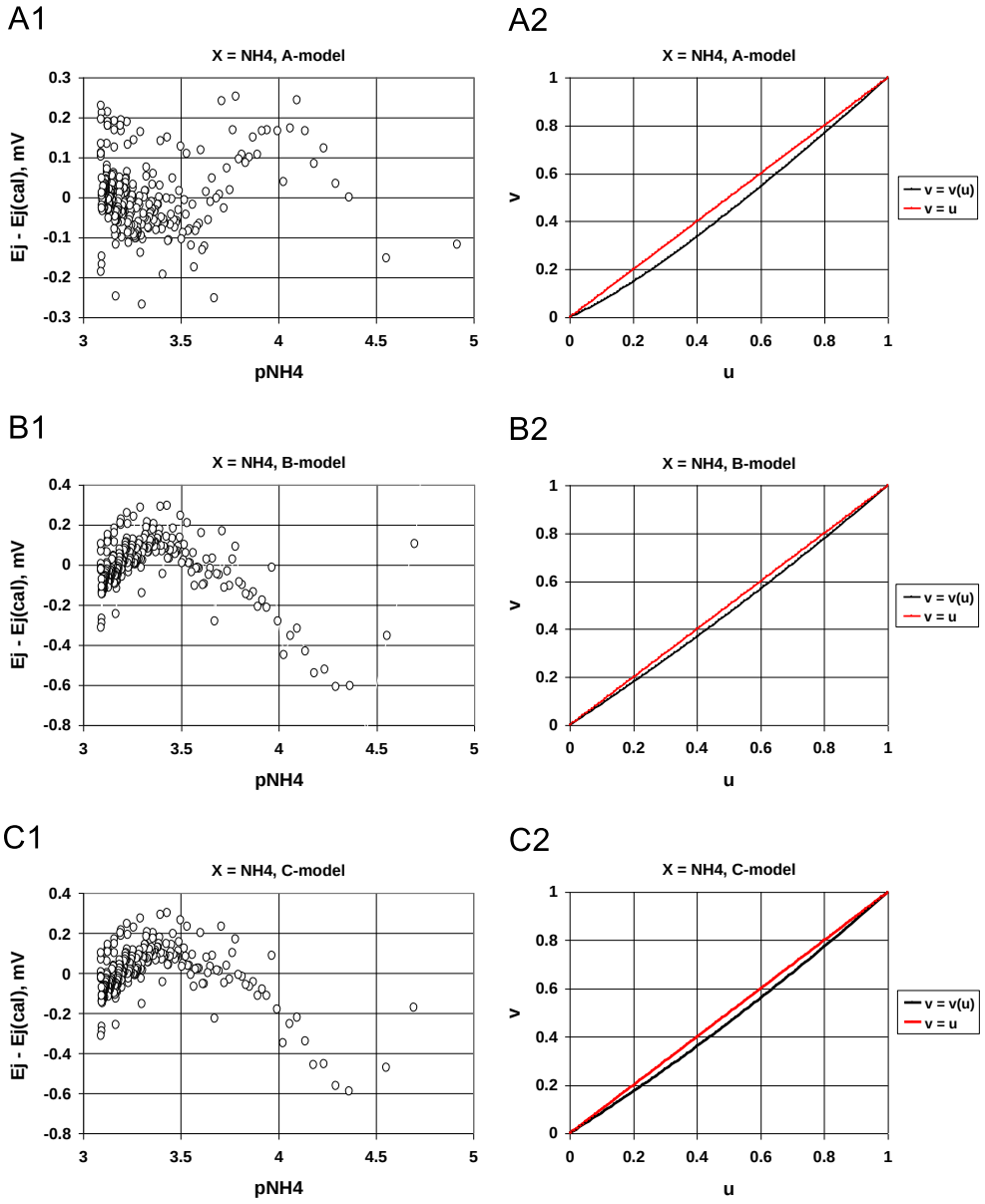

Fig. 3. The $E_j - E_j$ (cal) vs. pNH_4 relationships and plots within normalized variables obtained for the models A, B and C applied to NH_4-ISE calibration.

4.2. Results and discussion

The curves $E=E(pX)$ for (1°) X=NH_4, (2°) X=Ca, and (3°) X=F are presented in Fig. 2. The $\delta_j=E_j-E_j$ (cal) [mV] vs. pX relationships, where E_j (cal) is the $y=E$ value calculated according to particular models (A, B, C) at $V=V_j$, are presented for NH_4-ISE (Fig. 3), Ca-ISE (Fig. 4) and F-ISE (Fig. 5). The related plots were obtained on the basis of N experimental points, see Table 1. The related plots for $v=v(u)$ functions (5), (11) and (12) are presented in Figs. 3–5. As were stated below, within $u \in \langle 0, 1\rangle$ we have $u \geq v$ in 1° and 2°, and $v \geq u$ in 3°; see Eq. (16) and Fig. 2a, b, and c. In every instance, all internal points of the line $v=v(u)$ lie consistently on one side of the line $v=u$, irrespectively of the model applied. The values $\Omega=\Omega_A$, $\Omega=\Omega_B$ and $\Omega=\Omega_C$ related to models A, B and C, applied to calibration of NH_4-ISE, Ca-ISE and F-ISE, are collected in Table 2.

The degree of fit $\delta_j=E_j-E_j$ (cal) of the corresponding functions $E=E(pX)$ to experimental data (pX_j, E_j), see Eq. (21), is satisfactory, especially for F-ISE (Fig. 5). It should be noticed that $\delta_j=0.1$ mV corresponds to ΔpX ca. $0.1/60 \approx 0.0017$ for univalent ions. The δ_j values in acetate media were better (lower) than ones obtained in TISAB media (not presented in this paper). It testifies on account of usefulness of acetate buffer media for F-ISE confirmed in [30], although acetate ions have not, anyway, the complexing properties ascribed to components of TISAB [31,32]. It should be noted that $v \geq u$ for the curves $v=v(u)$ plotted for F-ISE, i.e. $\Omega_A=\Theta_A - ½$, $\Omega_B=\Theta_B - ½$, and $\Omega_C=\Theta_C - ½$.

Generally, the degree of fit is the best for the A-model, whereas it is somewhat worse for the B-model and the C-model applied to NH_4-ISE and Ca-ISE (Figs. 3 and 4). However, in the case of F-ISE, the models B and C are quite satisfactory (Fig. 5); the differences in fit of the corresponding curves are there quite insignificant. This results from the fact that F-ISE appears the best linearity among the ISE's considered in this paper, and then the Ω value is relatively small (see Table 2).

5. Final comments

In the paper [6] published lately, the rational functions of the Padé type were applied for the standard addition method (SAM).

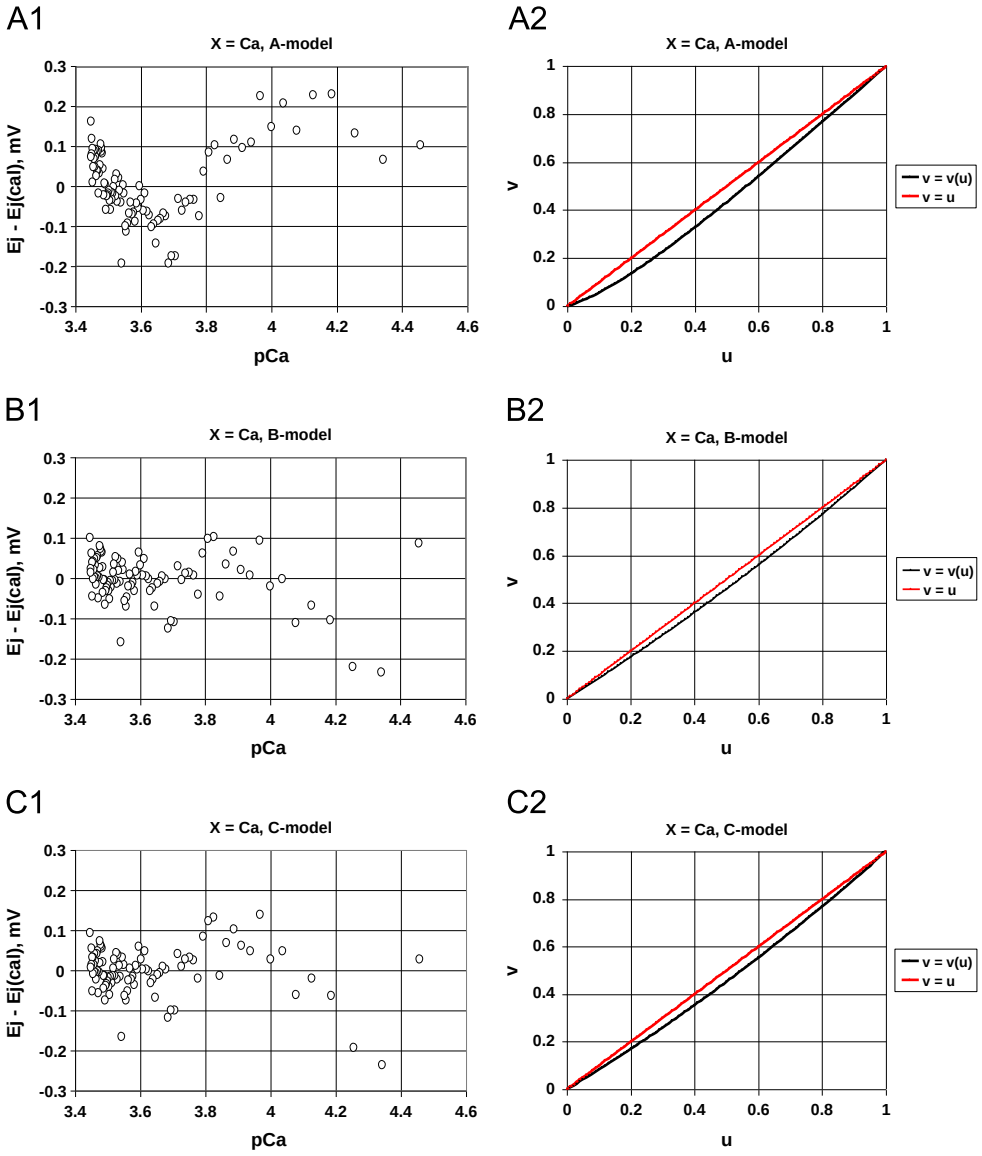

Fig. 4. The $E_j - E_j$ (cal) vs. pCa relationships and plots within normalized variables obtained for the models A, B and C applied to Ca-ISE calibration.

The relevant functions used for the calibration curves (CCM) contain the term a_0 in the models A, B and C, whereas in SAM the value $a_0=0$ is pre-assumed.

In the calculation procedure, a possible option to the (unweighted) LSM was an application of the weighed LSM (WLSM), i. e, an application of a heteroskedascity instead of homoskedascity postulate. However, the calibration points on the related graphs exceed only one decade of concentrations, e.g. ca. $4.5-3.4=1.1$ for $X_2=Ca$. From Fig. 4 we see that the error resulting from the mismatch of the model to experimental points is within ± 0.1 mV for the vast majority of experimental points, in the case where rational models, A or B, are used for the Ca-ISE. From the approximate formula $AE=0.03\bullet\Delta pX$ (with Nernstian slope assumed) it follows $\Delta pX=\pm 10^{-4}/(3\times 10^{-2})\approx 0.003$; this value is relatively small, even for a glass electrode (X=H) of high quality, where nominally $\Delta pH=\pm 0.001$, but ± 0.01 in practice. The biggest disadvantage of WLSM is the fact that the theory behind this method is based on the assumption that the weights are known exactly. This is almost never the case in real applications, of course, so estimated weights must be used instead. The weight expresses the precision of the information contained in the associated observation, at each data point. It is suggested that variances and then weights are based on replications, taking m replicate responses at each point x_j and then estimating the weights by the inverse of the sample variances. When the weights are estimated from small numbers of replicated observations, the results of an analysis can be very badly and unpredictably affected. If the number m of replicates is large, this procedure is inefficient in practice. Weighted least squares regression, like the other least squares methods, is also sensitive to the effects of outliers.

Different kinds of ISE, including divalent (Ca^{2+}) and monovalent (NH_4^+} cations, and monovalent anion (F^-) were considered and their characteristics expressed by calibration curves in concentration range exceeding one decade were considered. In reference to F-ISE and Ca-ISE, another models for calibration curve were applied in [22].

The normalization suggested in this paper provides a uniform, integral criterion of nonlinearity of curves obtained with use of different methods of analysis, within different ranges of concentrations assumed for standard solutions, and made under physicochemical conditions pre-assumed in the analysis. It appears to be far more general and more robust than the approaches to nonlinearity criteria suggested elsewhere; see e.g. [33] and references cited therein.

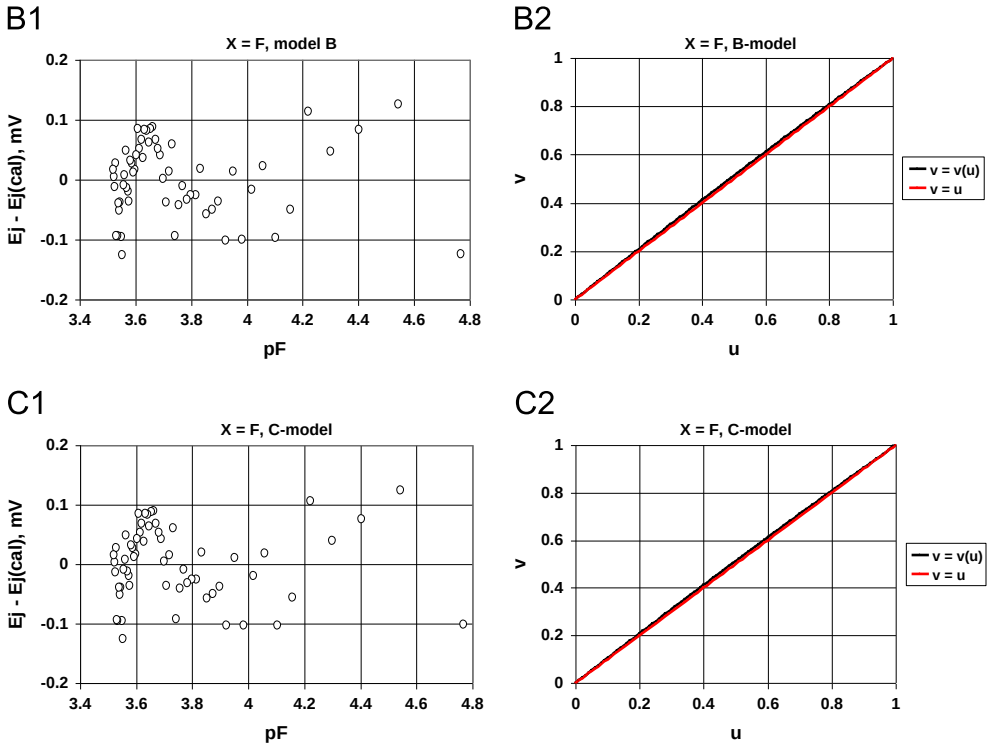

Fig. 5. The $E_j - E_j$ (cal) vs. pF relationships and plots within normalized variables obtained for the models B and C applied to F-ISE calibration.

Table 2
The Ω (Eq. (16)) values found for different X-IFE (X=NH_4, Ca, F) according to different models (A, B, and C).

Ω	NH_4-ISE	Ca-ISE	F-ISE
Ω_A	0.0417	0.0476	0.0087
Ω_B	0.0217	0.0269	0.0084
Ω_C	0.0271	0.0319	0.0082

Appendix A. Derivation of the formulas (5)–(8)

Setting $(x, y)=(x_1, y_1)$ into Eq. (2) we have

$$y_1 = \frac{a_0 + a_1 \cdot x_1 + a_2 \cdot {x_1}^2}{1 + a_3 \cdot x_1}, \text{ i.e. } y_1 + a_3 \cdot x_1 y_1 = a_0 + a_1 \cdot x_1 + a_2 \cdot {x_1}^2 \tag{A1}$$

Setting Eq. (4) into Eq. (2), and applying (A1) we obtain, by turns

$$y_1 + v \cdot \Delta y = \frac{a_0 + a_1 \cdot (x_1 + u \cdot \Delta x) + a_2 \cdot (x_1 + u \cdot \Delta x)^2}{1 + a_3 \cdot (x_1 + u \cdot \Delta x)} \tag{A2}$$

$$y_1 + a_3 \cdot x_1 y_1 + a_3 y_1 \cdot u \cdot \Delta x + v \cdot \Delta y + a_3 x_1 \cdot v \cdot \Delta y + a_3 \cdot u \cdot \Delta x \cdot v \cdot \Delta y = a_0 + a_1 \cdot x_1 + a_1 \cdot u \cdot \Delta x + a_2 \cdot {x_1}^2 + 2a_2 \cdot x_1 \cdot u \cdot \Delta x + a_2 \cdot u^2 \cdot (\Delta x)^2 \tag{A3}$$

$$a_3 y_1 \cdot u \cdot \Delta x + v \cdot \Delta y + a_3 x_1 \cdot v \cdot \Delta y + a_3 \cdot u \cdot \Delta x \cdot v \cdot \Delta y = a_1 \cdot u \cdot \Delta x + 2a_2 \cdot x_1 \cdot u \cdot \Delta x + a_2 \cdot u^2 \cdot (\Delta x)^2 \tag{A4}$$

Further transformation of Eq. (A4) gives Eq. (5), with α, β, and γ defined by Eqs. (6)–(8).

Transformation of formula (5) into (14)

$$v = \frac{\alpha \cdot u + \beta \cdot u^2}{1 + \gamma \cdot u} = \frac{\beta \cdot u(u + \alpha/\beta)}{\gamma \cdot u + 1} = \frac{\beta/\gamma \cdot u(\gamma u + \alpha\gamma/\beta)}{\gamma \cdot u + 1} = \frac{\beta/\gamma \cdot u(\gamma u + 1 + \alpha\gamma/\beta - 1)}{\gamma \cdot u + 1}$$

$$= \beta/\gamma \cdot u + \frac{\beta/\gamma \cdot u \cdot (\alpha\gamma/\beta - 1)}{\gamma \cdot u + 1} = \frac{\beta}{\gamma} \cdot u + \frac{\beta}{\gamma} \cdot \left(\frac{\alpha\gamma}{\beta} - 1\right) \cdot \frac{1}{\gamma} \cdot \frac{\gamma \cdot u + 1 - 1}{\gamma \cdot u + 1}$$

$$= \frac{\beta}{\gamma} \cdot u + \frac{1}{\gamma^2} \cdot (\alpha \cdot \gamma - \beta) \cdot \left(1 - \frac{1}{\gamma \cdot u + 1}\right) = \frac{\beta}{\gamma} \cdot u + \frac{\alpha \cdot \gamma - \beta}{\gamma^2} - \frac{\alpha \cdot \gamma - \beta}{\gamma^3} \cdot \frac{1}{u + 1/\gamma}$$

Transformation of formula (11) into (15)

$$v = \frac{\alpha \cdot u}{1 + \gamma \cdot u} = \frac{\alpha \cdot u}{\gamma \cdot u + 1} = \frac{\alpha}{\gamma} \cdot \frac{u}{u + 1/\gamma} = \frac{\alpha}{\gamma} \cdot \frac{u + 1/\gamma - 1/\gamma}{u + 1/\gamma}$$

$$= \frac{\alpha}{\gamma} \cdot \left(1 - \frac{1}{\gamma} \cdot \frac{1}{u + 1/\gamma}\right) = \frac{\alpha}{\gamma} - \frac{\alpha}{\gamma^2} \frac{1}{u + 1/\gamma}$$

Appendix B. Supporting information

Supplementary data associated with this article can be found in the online version at http://dx.doi.org/10.1016/j.talanta.2014.02.027.

References

[1] A.G. Asuero, A. Sayago, A.G. Gonzalez, Crit. Rev. Anal. Chem. 36 (2006) 41–49.
[2] R.M. Guion, Assessment, Measurement and Prediction for Personnel Decisions, Lawrence Erlbaum Associates, Inc, Mahwah, New Jersey, London (1998) 329.
[3] G. Baker, P. Graves-Morris, Pade Approximants (Encyclopedia of Mathematics and Its Implications), 2nd ed., Cambridge University Press, Cambridge, UK, 1996.
[4] E.B. Saff, Introduction to Padé approximants, Vanderbilt University, ⟨http://www-sop.inria.fr/miaou/anap03/PadeTalk.pdf⟩.
[5] W.H. Press, S.A. Teukolsky, W.T. Vettering, B.P. Flannery, Numerical Recipes in C. The Art of Scientific Computing, 2nd ed., Cambridge University Press, Cambridge (1999) 200–203 (Padé Approximants).
[6] K. Gorazda, A.M. Michałowska-Kaczmarczyk, A.G. Asuero, T. Michałowski, Talanta 116 (2013) 927–930.
[7] ⟨http://math.fullerton.edu/mathews/n2003/PadeApproximationBib.html⟩.
[8] A.I. Oleinick, D. Battistel, S. Daniele, I. Svir, C. Amatore, Anal. Chem. 83 (2011) 4887–4893.
[9] S. Dhatt, K. Bhattacharyya, J. Math. Chem. 51 (2013) 1467–1477.
[10] J.-P. Diard, B. Le Gorrec, C. Montella, J. Electroanal. Chem. 584 (2005) 182–191.
[11] A.M. Mainar, S.M. Garcia-Abarrio, A.M.F. Palavra, J.S. Urieta, J.I. Pardo, J. Chem. Eng. Data 56 (2011) 3818–3822.
[12] V.-M. Taavitsainen, Chem. Intell. Lab. Syst. 120 (2013) 136–141.

[13] I.C. Sánchez, J.S. Lee, J. Phys. Chem. B 113 (2009) 15572–15580.
[14] W.N. Focke, B. Du Plessis, Ind. Eng. Chem. Res. 43 (26) (2004) 8369–8377.
[15] T. Michałowski, Talanta 39 (1992) 1127–1137.
[16] T. Michałowski, E. Gibas, Talanta 41 (1994) 1311–1317.
[17] T. Michałowski, M. Ponikvar-Svet, A.G. Asuero, K. Kupiec, J. Solut. Chem. 41 (3) (2012) 436–446.
[18] T. Michałowski, A. Baterowicz, A. Madej, J. Kochana, Anal. Chim. Acta 442 (2001) 287–293.
[19] T. Michałowski, M. Toporek, M. Rymanowski, Talanta 65 (2005) 1241–1253.
[20] T. Michałowski, K. Kupiec, M. Rymanowski, Anal. Chim. Acta 606 (2) (2008) 172–183.
[21] M. Ponikvar, T. Michałowski, K. Kupiec, S. Wybraniec, M. Rymanowski, Anal. Chim. Acta 628 (2) (2008) 181–189.
[22] T. Michałowski, B. Pilarski, M. Ponikvar-Svet, A.G. Asuero, A. Kukwa, J. Młodzianowski, Talanta 83 (5) (2011) 1530–1537.
[23] S.D. Dimitrov, D.I. Kamenski, Comput. Chem. Eng. 15 (9) (1991) 657–662.
[24] L. Rajendran, Electrochim. Acta 51 (2006) 5407–5411.
[25] T. Michałowski, M. Rymanowski, Zakopane (2003) 444–449.
[26] T. Michałowski, M. Nizińska-Pstrusińska, M. Toporek, M. Rymanowski, Czas. Techn. 1-Ch/2004 (201) 71–83.
[27] ⟨http://en.wikipedia.org/wiki/Homotopy⟩.
[28] A. Jablari, H. Kheirl, A. Yildirim, Int. J. Numer. Method Heat Fluid Flow 23 (4) (2013) 692–706.
[29] J. Inczedy, Analytical Applications of Complex Equilibria, Horwood, Chichester, 1976.
[30] P. Kauranen, Anal. Lett. 10 (6) (1977) 451.
[31] M. Ponikvar, B. Sedej, B. Pihlar, B. Zemva, Anal. Chim. Acta 418 (1) (2000) 113–118.
[32] M. Ponikvar, V. Stibilj, B. Zemva, Food Chem. 103 (2) (2007) 369–374.
[33] K. Emancipator, M.H. Kroll, Clin. Chem. 39 (5) (1993) 766–772.